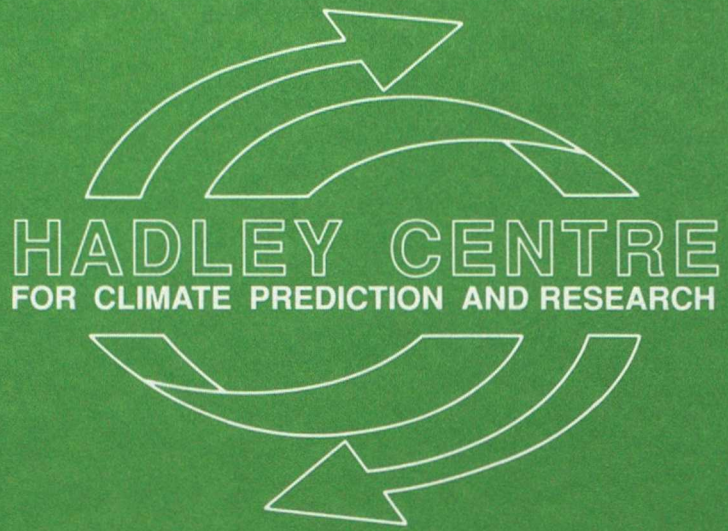

Stratospheric analyses provided by the U.K. Meteorological Office.

by

M. J. Bailey, A. O'Neill, V. D. Pope

CRTN 24 July 1992

CLIMATE
RESEARCH
TECHNICAL
NOTE

Hadley Centre
Meteorological Office
London Road
Bracknell
Berkshire RG12 2SY

Climate Research Technical Note No. 24

STRATOSPHERIC ANALYSES PRODUCED BY THE U. K. METEOROLOGICAL OFFICE

M.J. Bailey

A. O'Neill

R. Hooke Institute

and

V.D. Pope

Hadley Centre

July 1992

Hadley Centre for Climate Prediction and Research
Meteorological Office
London Road
Bracknell
Berkshire RG12 2SY
U.K.

Note: Permission to quote from this technical note should be obtained from the Director of the Hadley Centre.

Summary

Since late 1978, the U.K. Meteorological Office (UKMO) has processed accurate radiance measurements of the stratosphere from a set of three radiometers (SSU, MSU and HIRS) flown on satellites in the TIROS series. The radiometers scan both sides of the sub-satellite track giving almost global coverage. UKMO uses its own retrieval algorithm to derive thicknesses from radiances. The retrieval is a linear, physical-statistical method which utilizes a reference set of temperature profiles as *a priori* data. Thicknesses are added to a contemporaneous field of geopotential height at 100 HPa to give geopotential heights at standard pressure levels in the stratosphere up to 1 HPa. Global synoptic fields for 12 GMT are produced every day on a regular latitude-longitude grid by linear interpolation in space and time. The paper describes the retrieval method and objective analysis in detail. It outlines the availability of data in the 12-year archive, and summarizes the main findings of several studies on data quality. Finally, it tells prospective users how to get the data, and what checks they should make before trying to interpret them.

1. Introduction

Since 1978, routine measurements of the troposphere and stratosphere have been made by the TIROS Operational Vertical Sounder (TOVS) on board the NOAA series of operational satellites. The TOVS system comprises three instruments which scan in swathes across the sub-satellite track: a Stratospheric Sounding Unit (SSU), which provides the best vertical resolution of the stratosphere, a High Resolution Infrared Sounder (HIRS) and a Microwave Sounding Unit (MSU). Pick and Brownscombe (1981) describe the SSU in detail; Schwalb (1978) describes the TOVS system as a whole.

The TOVS data are processed by the National Environmental Satellite Data and Information Service (NESDIS) in the U.S.A.. Besides applications in weather forecasting for the troposphere and lower stratosphere, TOVS data are used to construct synoptic maps for research in stratospheric meteorology. Both the National Meteorological Center (NMC) in the U.S.A. and the Meteorological Office (UKMO) in the U.K. produce global analyses of thickness, temperature and geopotential height at standard pressure levels throughout the stratosphere. This paper describes UKMO's stratospheric analyses, which have been produced since December 1978 (NMC's start a few months earlier), and will continue to be produced, barring instrument failure, until the TOVS system is replaced by Advanced Microwave Sounding Units in the mid 1990s. The paper details the method of analysis (section 2), disusses data availability and quality (section 3), and gives some guidance to prospective users (section 4). Data formats are given in the appendix.

Although TOVS radiances form the basis of both sets of analyses, subsequent processing of the data is somewhat different at the two centres. In brief, NESDIS retrieve temperatures from radiances by using co-located satellite and in situ data, the latter being updated weekly for the 1000 - 10 HPa region (Phillips et al. 1979). Above the 10 HPa level, an historical temperature record is used because there is very little *in situ* data. NESDIS provide NMC with layer-mean temperatures which are used in conjunction with NMC's operational analysis of geopotential height at 100 HPa to produce gridded fields of temperature and geopoential height up to 0.4 HPa. UKMO, on the other hand, directly converts TOVS radiances obtained from NESDIS to deep layer-mean thicknesses by using its own retrieval method, developed by Campbell and Pick (1979). This is a linear, physical-statistical technique which utilizes an historical record of

temperature profiles derived from rockets. The thicknesses are gridded, and are then added to UKMO's operational analysis of geopotential height at 100 HPa which are then smoothed to produce gridded fields of geopotential height up to 1 HPa. (Note that these analyses should be distinguished from those that have been produced recently at UKMO by assimilating thicknesses retrieved from TOVS radiances into a general circulation model; see section 4.)

The following data are archived at UKMO and are available for research:
1. Radiances in swathes across the orbital track of the satellite. Radiances from 11 channels of the TOVS system are available at 4 viewing angles about the nadir direction (at 10° and 30° either side of nadir): all three SSU channels, six HIRS channels and two MSU channels.
2. Thicknesses of the 100-20, 100-10, 100-5, 100-2 and 100-1 HPa layers at 4 viewing angles about the nadir direction.
3. Synoptic maps of radiances on a global, latitude-longitude grid.
4. Synoptic maps of geopotential height on the same grid for the levels 850, 500, 300, 200, 100, 50, 20, 10, 5, 2, 1 HPa.
Formats of these datasets are given in the appendix.

UKMO's analyses have formed the basis of several studies of stratospheric meteorology and dynamics. For instance, isentropic maps of Ertel's potential vorticity derived from the analyses were used by McIntyre and Palmer (1983) to identify planetary-wave breaking in the stratosphere. Hirota et al. (1983) studied aspects of the seasonal evolution of the stratosphere; Ziemke and Stanford (1991) the long-period response at high latitudes to tropical forcing; and Fairlie and O'Neill (1988) made a dynamical study of a major stratospheric warming. The data have been sent to experimentalists to support ground-based measurement campaigns, and form part of the data used by the Free University of Berlin to issue alerts for stratospheric warmings ("stratalerts").

Investigators in the U.K. can get the data from the Geophysical Data Facility at the Rutherford/Appleton Laboratory. Others should contact the UKMO directly.

2. Retrieval and analysis of TOVS radiance measurements

2.1 The measurements

NOAA satellites fly in sun-synchronous orbits at a height of 850 km, making about 14 orbits per day. At any one time, there are generally 2 satellites providing data; these data are analysed independently. One satellite is designated the primary spacecraft (the one with the better coverage of the stratosphere), and analyses for outside users are usually available only for this satellite.

Analyses of stratospheric thicknesses and geopotential heights are produced by an objective method which makes use of radiances measured by 8 channels of the TOVS system: channels 25, 26 and 27 of the SSU; channels 23 and 24 of the MSU; and channels 1, 2 and 3 of the HIRS. All three instruments scan across the orbital path to both sides of nadir, though with different scan patterns. The SSU scans at angles of 35°, 25°, 15° and 5° to both sides of nadir. This scanning feature leads to much better horizontal resolution than would be afforded by a fixed angle device. In the analysis, HIRS and MSU measurements are interpolated for convenience onto the same fields of view as the SSU. Figure 1(a) shows the area of the Earth covered by the SSU. With side-scanning, measurements extend to 87° in latitude in both hemispheres. Coverage is best at high latitudes where measurements overlap substantially, giving almost complete coverage over a 24-hour period. (Between 45° and 87° latitude, coverage exceeds 70% at each latitude.) Coverage is worst near 30° latitude where ascending and descending orbits cross, giving a zonal resolution only of scales larger than about wavenumber 7.

The vertical coverage of the three instruments is illustrated in Fig. 1(b), which shows the weighting functions of channels used in the analysis. The three channels of the SSU have weighting functions centred in the middle and upper stratosphere near 15, 5 and 1.5 HPa; the two MSU channels have weighting functions centred in the lower stratosphere; and the three HIRS channels have broad weighting functions spanning much of the stratosphere. Statistical tests indicate that the effective vertical resolution is about 10 km in the stratosphere.

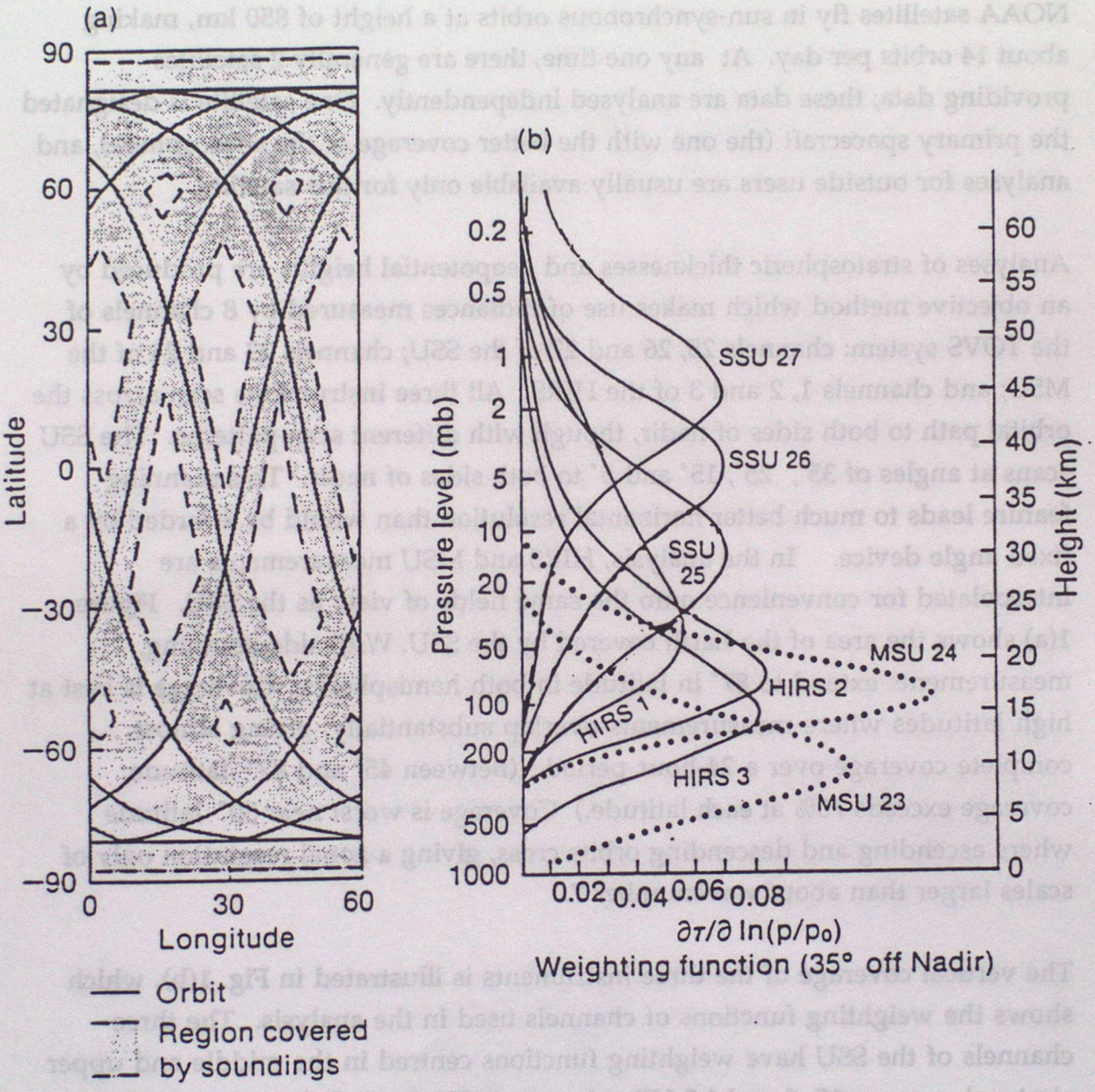

Figure 1 (a) Region covered by observations from an SSU over 24 hours in a 60° wide longitudinal band from the north to the south pole. (b) Weighting functions (at 35° off nadir) for SSU, MSU and HIRS channels used to retrieve thicknesses (adapted from Pick and Brownscombe 1981).

2.2 Thickness retrievals and method of analysis

From each sounding of 8 measured radiances, 5 deep-layer thicknesses are retrieved for the stratosphere: viz 100-20, 100-10, 100-5, 100-2 and 100-1 HPa. Thicknesses rather than temperatures are retrieved because of the inherently low vertical resolution of the TOVS data. There are two stages in the analysis: a preparatory first stage in which a linear equation is derived giving thicknesses in terms of radiances; and an operational second stage in which the equation is used to retrieve thicknesses from measured radiances. Retrieved thicknesses lie in swathes across the sub-satellite track (Fig. 1(a)). Interpolation in space and time produces synoptic maps on a regular grid. Geopotential heights are then obtained by adding thicknesses to an independently analysed field of geopotential height at 100 HPa.

Stage 1: computation of regression coefficients

To find an linear equation giving thicknesses in terms of radiances, a representative selection of temperature profiles measured by rockets was utilized. The rocket profiles were a reference set of 1200 profiles obtained from the Upper Air Branch of NOAA/NMC. They included profiles representative of winter warming conditions. To reduce the range of atmospheric conditions that had to be covered by the expression, the rocket profiles were divided into 7 zones, and the expression was obtained for each zone separately. There were three latitudinal zones in the extra tropics in winter (each 20° wide), three in summer, and one tropical zone (60° wide) for the whole year. The zoning did not distinguish between hemispheres, biasing the *a priori* data in favour of the northern hemisphere where most of the rocket ascents took place.

For each temperature profile, the 5 thicknesses listed above were calculated by using the hydrostatic equation. The next step was to calculate the 8 radiances that would have been measured in a coincidental satellite sounding, the so-called simulated radiances. The calculation required knowledge of the combined transmission of atmosphere and radiometer channel, which was derived for each pairing of channel and rocket profile by the approximate method outlined in the Annex.

The following (zone-dependent) linear relationship was assumed between each set of 5 thicknesses, denoted by a column matrix x, and the corresponding set of 8 simulated radiances, denoted by a column matrix y:

$$x - x_m = D\,(y - y_m) \qquad (1)$$

where **D** is a rectangular matrix to be determined, and where x_m and y_m are the means of the thicknesses and simulated radiances for each zone. Thicknesses and simulated radiances were calculated for each of the rocket profiles and substituted into Eq. (1), giving an overdetermined set of equations for the unknown matrix **D**. A regression analysis gave a best estimate of **D** (in a least-squares sense); its elements, called regression coefficients, were found to vary reasonably smoothly from zone to zone.

D was recalculated for each new satellite, and also if there was a change in the number of operational channels in the TOVS system, or if an SSU cell pressure changed by more than 10% - table 1 gives dates of these changes. A correction for a change in cell pressure was made as follows. For each channel of the SSU, transmittances were computed at the nominal cell pressure and at a cell pressure 10% greater. The transmittance at the actual cell pressure of an affected channel was then estimated by linear extrapolation. After July 1980, an additional correction was made to allow for the Earth's curvature.

To simplify the operational retrieval of thicknesses, the matrix **D** was derived for simulated radiances corresponding to a (fictitious) nadir viewing angle. To use Eq. (1) with off-nadir radiances measured operationally, they must be corrected (the weighting functions for off-nadir views are shifted upward with respect to those at nadir). The corrected radiances are estimates of the radiances that would have been measured by a nadir sounding taken over the patch of the Earth's surface seen in an off-nadir view. The HIRS and MSU radiances were nadir corrected at NOAA/NESDIS; the SSU radiances were corrected at UKMO as follows.

Spacecraft name	Initial month		cell pressure Ch 26.	Ch. 27
Nominal cell pressure (mb)			35.60	10.82
NOAA-7	April	1983	x	x
NOAA-8	May	1983	x	x
NOAA-8	November	1983	x	xx
NOAA-8	February	1984	x	x
NOAA-6	February	1985	x	xx
NOAA-9	April	1985	xx	*
NOAA-9	October	1985	xx	*
NOAA-11	November	1988	xx	xx

Key:

x Change of 10-20%
xx Change of 20-30%
* Change of 50-60%

Table 1: SSU cell pressure changes. The table indicates changes in cell pressure of more than 10% for the SSU channels for the prime spacecraft used in the analysis. SSU channel 25 remains within 10% of the nominal cell pressure of 108.18 mb.

A linear equation was assumed relating a set of 8 radiances **y*** measured at a particular off-nadir viewing angle to the corresponding set of 8 radiances **y** that would have been measured at nadir:

$$\mathbf{y^* - y = C^* y^* + c^*} \qquad (2)$$

where **C*** and **c*** are respectively square and column matrices, which depend on the viewing angle. Simulatated radiances **y** and **y*** were calculated for each of the rocket temperature profiles, and substituted into Eq. (2), giving an overdetermined set of equations for **C*** and **c***. A regression analysis gave a best estimate of the matrices (in a least-squares sense) for each viewing angle. With these matrices, radiance corrections (**y*** - **y**) may be determined from actual off-nadir radiance measurements **y***. Subtracting these corrections from **y*** gives the nadir-corrected radiances **y**. **C*** and **c*** are recalculated for each new satellite, and also if there is a change in the number of operational SSU channels, or if SSU cell pressures change by more than 10% (see table 1 for dates). Campbell and Pick (1979) showed that the top channel (27) of the SSU was least well corrected.

Stage 2: routine processing of measured radiances

Data supplied by NOAA have HIRS measurements interpolated onto the same orbital grid as those of MSU. These data are then processed routinely at UKMO in the following steps:

1. **Interpolation of HIRS and MSU data.** HIRS and MSU radiances are first interpolated onto SSU fields of view by locating the nearest 4 HIRS/MSU radiances to each SSU viewing position. In effect, the three instruments now provide data at the common viewing angles of 5°, 15°, 25° and 35° off nadir.

2. **Quality control.** A "spike check" is made by taking the mean and standard deviation of all radiances in a block of data. All radiances greater than three standard deviations from the mean are rejected.

3. **Grouping into "superobs".** The 8 x 8 fields of view of the HIRS/MSU/SSU are grouped into 4 x 4 fields of view by combining 4 adjacent observations (or 3 if one field of view is missing) into one observation known as a "superob". The superob fields of view are centred at angles of 30° and 10° on both sides of nadir. The superob is rejected if quality control rejects any one of the radiances used to create it.

4. **Nadir corrections.** The pre-computed matrices $\mathbf{C}^*$ and $\mathbf{c}^*$ for superob viewing angles are used in Eq. (2) to correct superob SSU radiances $\mathbf{y}^*$ to a nadir view (HIRS and MSU radiances are received as corrected values). A standard nadir correction is applied if data from a channel is missing in a superob (in which case, the matrices do not apply as computed).

5. **Retrieval of thicknesses.** For each nadir-corrected radiance $\mathbf{y}$, pre-computed values of $\mathbf{D}$, $\mathbf{x_m}$ and $\mathbf{y_m}$ are chosen according to latitude band. To allow for time of year, these values are varied sinusoidally between winter and summer. Thicknesses $\mathbf{x}$ for the standard layers 100-20, 100-10, 100-5, 100-2, 100 -1 HPa are then obtained from:

$$(\mathbf{x} - \mathbf{x_m}) = \mathbf{D}\,(\mathbf{y} - \mathbf{y_m}) \qquad (3)$$

6. **Interpolation onto a global grid at 12 GMT.** Both radiances y and retrieved thicknesses x are then interpolated linearly in space and time from the superob fields of view onto a global grid of 5° latitude by 5° longitude at 12 GMT (0 GMT before 3 August 1979). The value at a grid point is influenced by observations within 500 km and within 12 hours of 12 GMT. Jackson et al. (1990) experimented with the space-time interpolation and found little change in gridded fields when using different interpolation methods and search windows.

7. **Filling in missing values.** Because of missing radiance measurements, a grid point may have no values attributed to it. In this case, a search is made within 20 grid lengths for grid points with attributed data. If successful, linear interpolation is then used; if unsuccessful, a mean value for the whole grid is used. N.B. The number of missing grid points is recorded as header information on the stored data (see appendix for details). If more than 650 grid points are missing, that day's analysis should be discarded.

8. **Analysis of geopotential height.** Global fields of geopotential height for the stratosphere are constructed by adding the gridded thicknesses to an objective analysis of geopotential height at 100 HPa. The analysis comes from a centre for operational weather forecasting (currently UKMO; see section 3 for details). The same source provides fields of geopotential height at 50 HPa and also at tropospheric levels. Geopotential heights are thereby obtained at 850, 500, 300, 200, 100, 50, 20, 10, 5, 2 and 1 HPa. (Geopotential heights at 200 HPa are not analysed on the same footing as other tropospheric levels, but are derived by linear interpolation in the vertical.)

9. **Smoothing.** The gridded fields of radiances, thicknesses and heights are then smoothed in the horizontal by Fourier analysis. Zonal wavenumbers greater than 12 are discarded, and Fourier coefficients of remaining zonal wavenumbers are smoothed by discarding pole-to-pole wavenumbers greater than 12. The smoothing is a compromise between the almost complete spatial coverage at high latitudes and the poorer coverage where ascending and descending orbits cross at low latitudes.

3. Data sources, availability and data quality

3.1 Data sources and availability of radiances and retrieved thicknesses

At any one time, there are usually two NOAA satellites making measurements. The one giving better stratospheric data is designated as the prime satellite by UKMO. Table 2 and figure 2 show the time periods covered by the prime satellite from December 1978 to the present. On some of the satellites, one or more of the TOVS channels did not work, as indicated in the table and on the figure. Users should have this figure at hand when interpreting the data, since a missing channel can significantly reduce the vertical resolution of analysed fields. Figure 3 shows for each month the number of days in the prime archive when an analysis was not made (for various technical reasons), or when the analysis was felt to be unreliable because of data gaps.

Usually, only data from the prime satellite are disseminated to outside users. However, data from the secondary satellite are also archived, and can be made available to serve as a check on data quality. Figure 4 shows the time periods covered by all satellites in the NOAA series; data from the prime satellite are usually backed up by data from the secondary satellite.

3.2 Source of tropospheric analyses

The source of tropospheric analyses of geopotential heights, including the 100 HPa tie-on field, has changed over the years. Table 3 and figure 5 give the sources and the periods covered by them. Analyses provided by the European Centre for Medium Range Weather Forecasts (ECMWF) were their global analyses of FGGE data. UKMO(NH) denotes tropospheric analyses north of 20° N, which were made at UKMO using the now defunct "octagon" forecast model. The first global analyses used at UKMO to produce stratospheric analyses operationally were supplied by NMC. They were replaced by analyses from UKMO's first global forecast model (denoted GL on the figure), and are currently obtained from the recently introduced "Unified Model" (UM).

Spacecraft name	Spacecraft number	Initial month		data used
TIROS-N	1	December	1978	'RAW' minus SSU 27
NOAA-6	2	November	1979	'RAW'
NOAA-6	2	March	1980	'PRC' minus MSU 23
NOAA-7	4	April	1983	'PRC'
NOAA-8	6	June	1983	'PRC' minus SSU 27 (7/12/83 to 17/12/83)
NOAA-7	4	June	1984	'PRC' minus SSU 26
NOAA-6	2	March	1985	'PRC' minus HIRS (N.B. s/c 2 gains MSU
NOAA-9	5	April	1985	'PRC'
NOAA-9	5	March	1987	'PRC' (1/3/87 - 8/3/87 inc) no data (9/3/87 - 15/3/87 inc) 'RAW' (16/3/87 - 31/3/87)
NOAA-9	5	April	1987	'RAW'
NOAA-9	5	April	1988	'PRC' minus 23 (heights) 'RAW' (radiances)
NOAA-9	5	September	1988	'PRC' minus MSU 23 also minus MSU 21, 22 from 12/9/ 88
NOAA-11	8	November	1988	'PRC'

Key
Spacecraft name: name usually used to identify the satellite
Spacecraft number: number used as an identifier in the datasets produced by UKMO (see appendix).
'PRC' (processed) data = HIRS 1 2 3 MSU 23 24 SSU 25 26 27 radiances obtained from NOAA
'RAW' data = SSU 25 26 27 radiances derived at UKMO from instrument signal data.

Notes
Heights datasets

April 1983	s/c 2 1st to 5th, s/c 4 6th to 30th

Radiance datasets

April 1982	s/c 2 MSU 23 regained 26th (not used in heights until 1985). Also on 26th MSU 212 and 22 regained, HIRS 9 and 17 lost.
April 1983	s/c 2 1st to 16th, s/c 4 17th to 30th.
May 1983	s/c 4 1st to 24th. MSU 21 and 22 replace HIRS 9 and 17. s/c 6 25th to 31st. HIRS 9 and 17 replace MSU 21 and 22, no SSU 27.
June 1983	s/c 6 SSU 27 regained 16th. MSU 21 and 22 replace HIRS 9 and 17 on 17th.

Table 2 Monthly heights and radiance spacecraft.

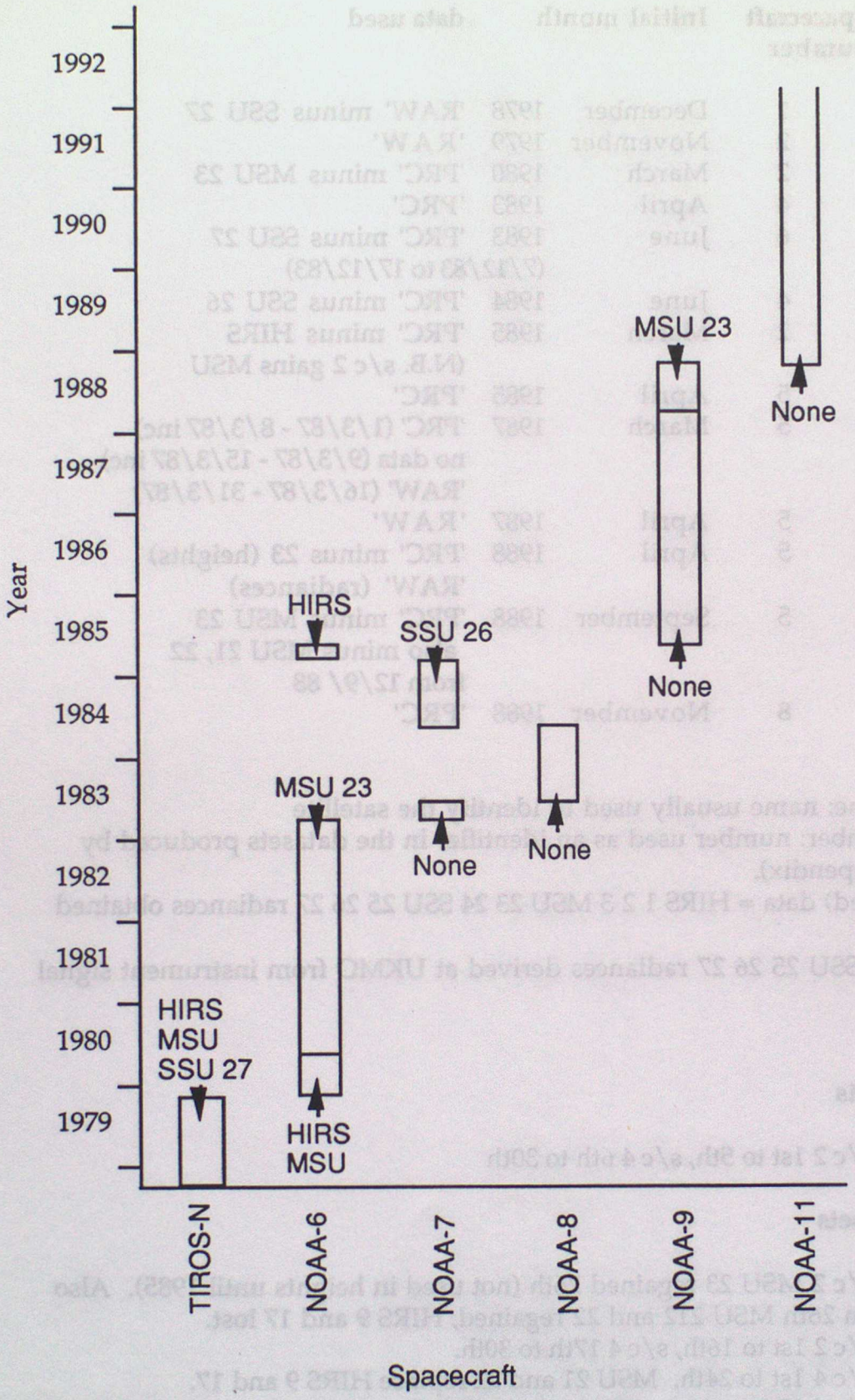

Figure 2 Sources of satellite data used to create prime archive of radiances and geopotential heights. Missing radiometer channels are indicated.

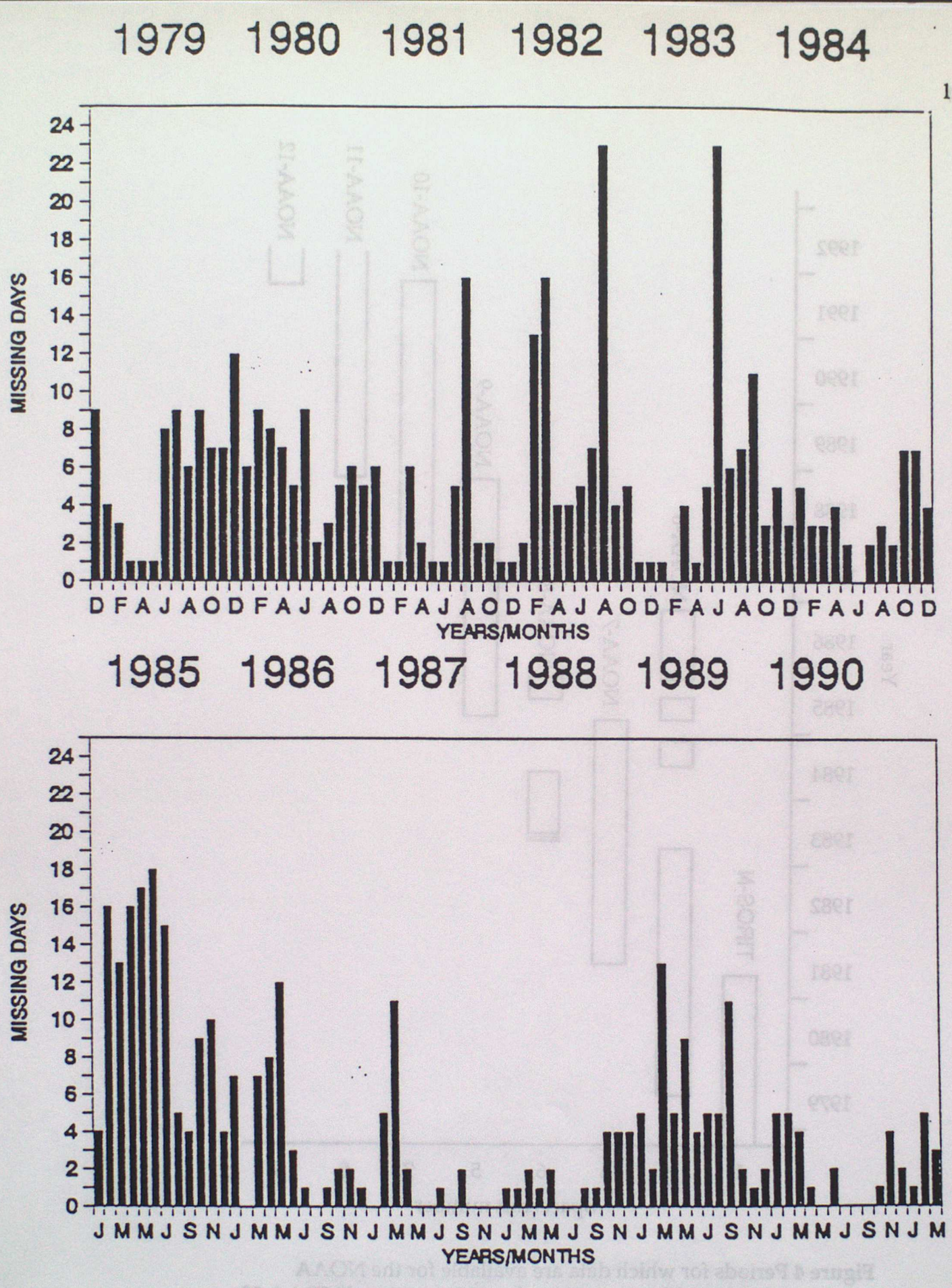

Figure 3 Number of missing days or days with inadequate data in each month in UKMO's archive for the stratosphere

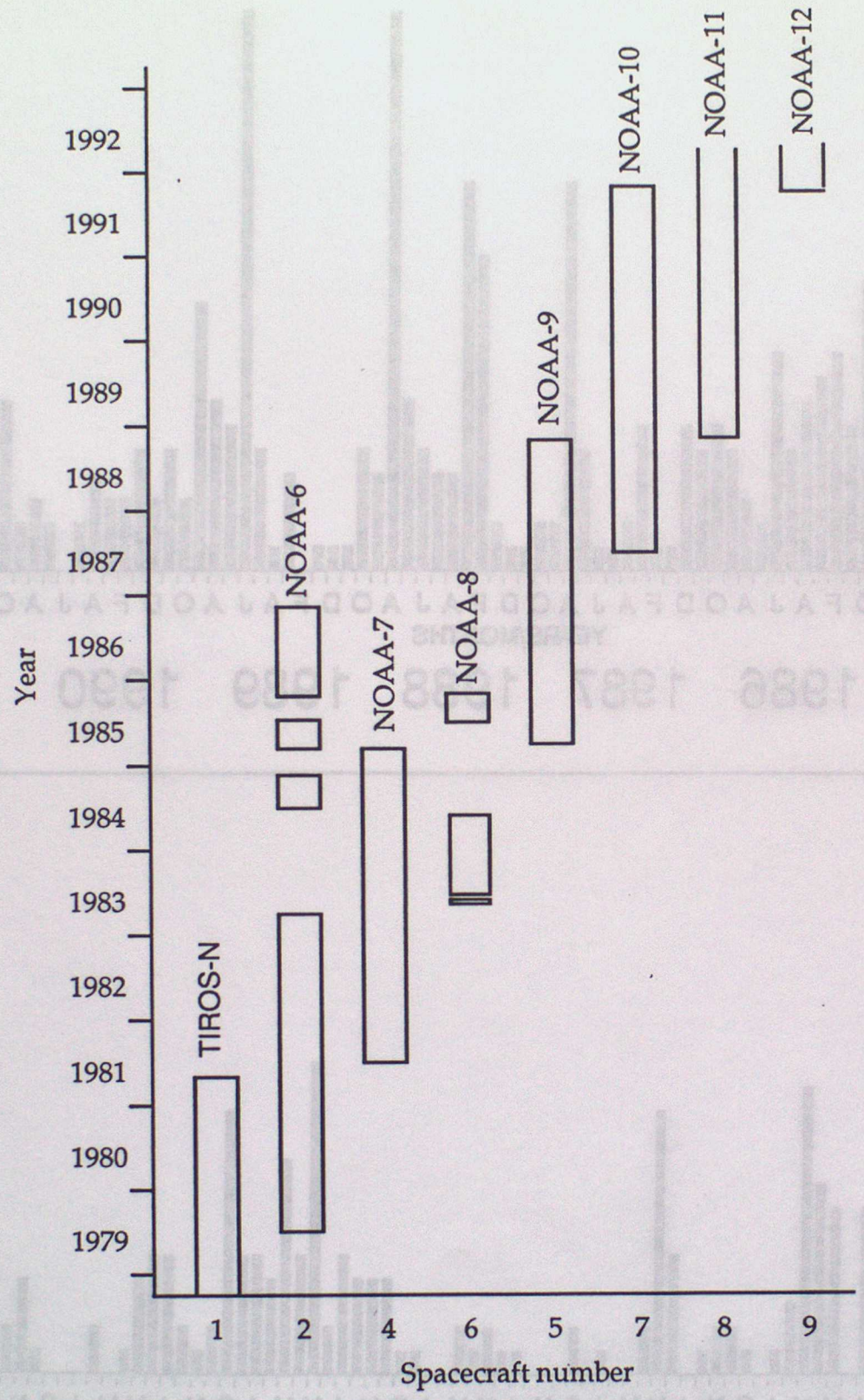

Figure 4 Periods for which data are available for the NOAA satellites in the TIROS series. Note that NOAA-10 and NOAA-12 do not have an SSU. The spacecraft number is the number used in the UKMO data to identify the satellite (see appendix).

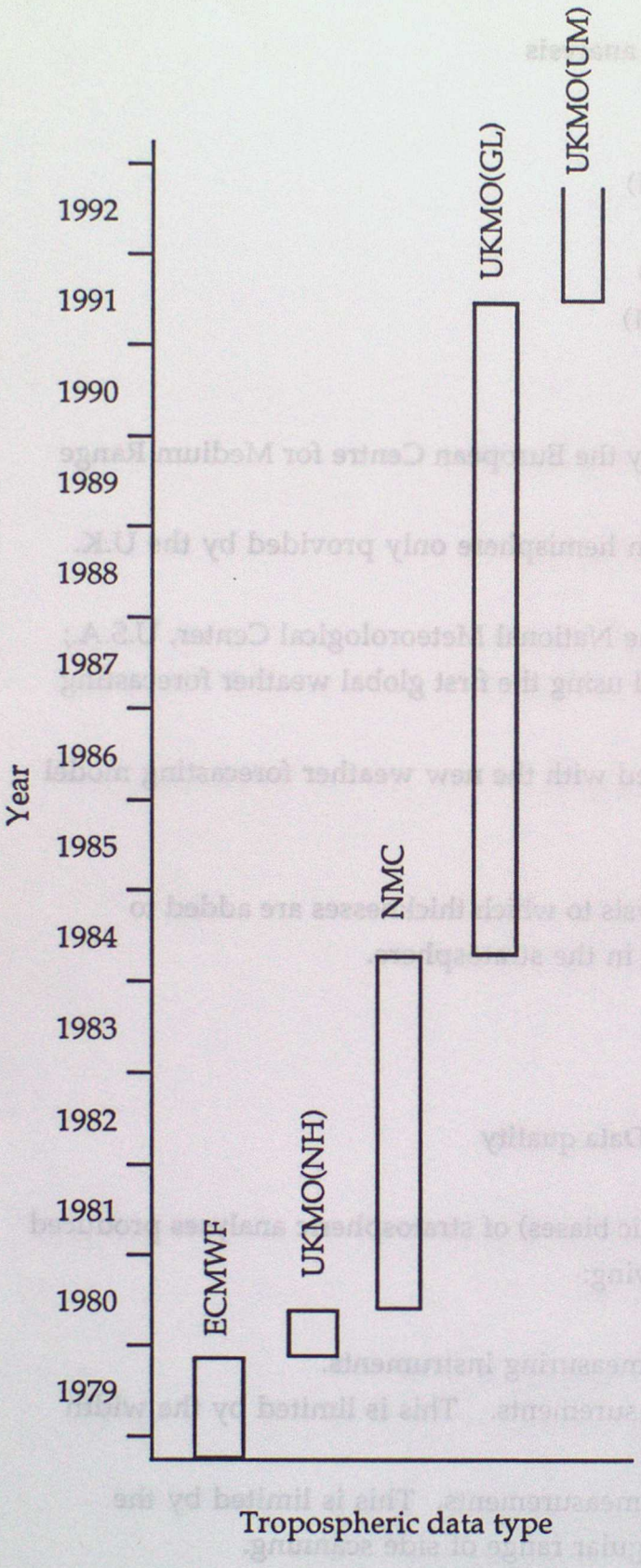

Figure 5 Source of the 100 HPa analysis to which thicknesses are added to produce fields of geopotential height in the stratosphere. See table 3 for key.

Date	Source of 100 HPa analysis
1 December 1978	ECMWF
1 December 1979	UKMO(NH)
1 March 1980	NMC
1 April 1984	UKMO(GL)
12 June 1991	UKMO(UM)

Key

ECMWF: FGGE analyses produced by the European Centre for Medium Range Weather Forecasts;
UKMO(NH): analysis for the northern hemisphere only provided by the U.K. Met Office;
NMC: global analyses provided by the National Meteorological Center, U.S.A.;
UKMO(GL): global analyses produced using the first global weather forecasting model (now defunct) at UKMO;
UKMO(UM): global analyses produced with the new weather forecasting model at UKMO, the "Unified Model".

Table 3: Source of the 100 HPa analysis to which thicknesses are added to produce fields of geopotential height in the stratosphere.

3.3 Data quality

The accuracy (precision and systematic biases) of stratospheric analyses produced by UKMO is influenced by the following:

1. The accuracy and stability of the measuring instruments.
2. The vertical resolution of the measurements. This is limited by the width and overlap of weighting functions.
3. The horizontal resolution of the measurements. This is limited by the number of satellite orbits and the angular range of side scanning.
4. The retrieval method which derives thicknesses from radiances. The reference *a priori* data used in the retrieval cannot represent the full range of stratospheric conditions.

5. The interpolation of observations. Errors inevitably arise when observations from orbits spread throughout the day are interpolated onto a regular latitude - longitude grid at a specified synoptic time.
6. The accuracy of the 100 HPa analysis which is used as a base level. Though operational weather forecasting centres such as the UKMO continue to improve their tropospheric analyses, errors remain as evidenced by differences between independently produced fields, particulary in the southern hemisphere where ground-based data are sparse.

The effect of each of these factors is difficult, if not impossible, to assess definitively given the limited amounts (or complete lack of) independent data for the middle and upper stratosphere. Moreover, the reliability of derived fields is strongly influenced locally by the vertical and horizontal scales of the actual circulation; representative error values, such as are quoted below, should serve only as a guide, never as a stamp of approval.

(a) Comparison with radiosondes, rocketsondes and lidars

The accuracy of TOVS radiance measurements has been discussed by Phillips et al. (1979), Smith et al. (1979) and by Pick and Brownscombe (1981). Nash and Brownscombe (1983), Nash and Forrester (1986) and Nash and Edge (1989) considered the precision of the radiances measured by the SSUs, which they evaluated by laboratory tests and by monitoring the instruments in orbit. Nash and Brownscombe found that SSU radiance measurements had a relative error of less than 0.2 K in equivalent brightness temperature. This error is small enough for radiance measurements to detect small rises in temperature (of about 1 K) due to injections of volcanic aerosol into the stratosphere (Nash, personal communication). Nash and Edge remarked that for long-term monitoring of temperature with SSU radiances, spectroscopic drift corrections are necessary to correct for changes in the pressure (due to small leaks) in the pressure modulator cells. At UKMO, corrections have been made as detailed in section 2.2.

Nash and Brownscombe (1983) compared SSU radiances with radiances derived from temperature measurements made by rockets. They concluded that SSU radiances were at least as accurate as those derived from rockets; indeed, they suggested that the SSU could be used to cross-validate rocket measurements. Jenkins et al. (1987) showed that radiances synthesized from lidar measurements of temperature agreed very well (to within about 1 K in brightness temperature)

with those measured by an SSU. These comparisons demonstrate that limitations of resolution and analysis method, rather than radiometric errors, are the prime cause of errors in final gridded analyses.

Routine comparisons of UKMO's gridded analyses with measurements from radiosondes and rocketsondes indicate that typical differences in geopotential heights at 10 HPa are 50 to 100 m (Pick and Brownscombe 1981). (Typical amplitudes for planetary-scale disturbances in the middle atmosphere are ten times this value.)

However, bigger differences are found during major warmings. Figure 6 shows a map of geopotential height during a major warming produced by UKMO, together with a corresponding map produced by Prof. Labitzke's group at the Free University of Berlin. (The latter map is produced by subjective analysis of the data, and will also suffer from error, particularly above the lower stratosphere where in situ data become sparse.) Differences between the maps are large in places - about 500 m at the pole. During major warmings, there may also be substantial differences locally between vertical temperature profiles inferred from satellite data and those measured by radiosondes, rocketsondes or lidars. Although the satellite data has the important advantage of horizontal coverage, the downward-looking instruments may be unable to capture sharp changes in vertical temperature gradients, such as are found in narrow baroclinic zones during strong warmings in the stratosphere (Fairlie et al. 1990).

(b) Comparison of independent TOVS systems

A stringent test of the quality of the analyses is the degree of day-to-day continuity in fields of Ertel's potential vorticity (EPV). EPV should be conserved for a few days at least in the middle and lower stratosphere where the radiative damping time is about a week or more. Sudden changes in the values of maxima or minima on a sequence of isentropic maps of EPV are likely to indicate errors in the fields. Moreover, temperature fields must be differentiated twice to calculate EPV, and this highlights differences between fields of different origin.

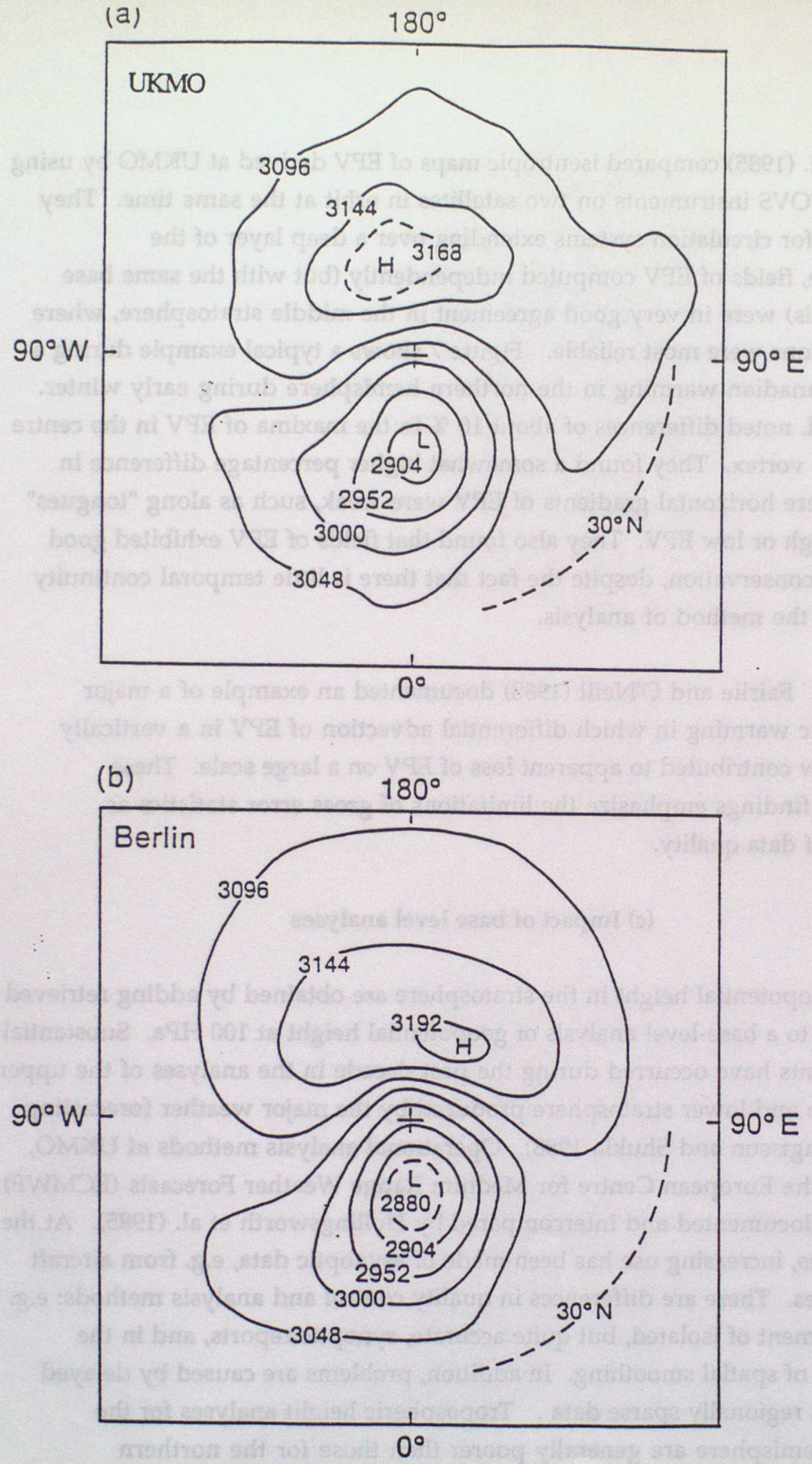

Figure 6 Polar-stereographic maps of geopotential height for the northern hemisphere at 10 HPa on 5 February 1981. Units: dam with contour interval 48 dam. Intermediate contours are dashed. (a) Analysis produced by UKMO using TOVS data and an analysis of geopotential height at 100 HPa. (b) Subjective analysis produced by the Free University of Berlin using radiosonde and rocket data (adapted from Labitzke et al. 1981).

Clough et al. (1985) compared isentropic maps of EPV derived at UKMO by using data from TOVS instruments on two satellites in orbit at the same time. They found that, for circulation systems extending over a deep layer of the stratosphere, fields of EPV computed independently (but with the same base level analysis) were in very good agreement in the middle stratosphere, where the calculations were most reliable. Figure 7 shows a typical example during a so-called Canadian warming in the northern hemisphere during early winter. Clough et al. noted differences of about 10 % in the maxima of EPV in the centre of the polar vortex. They found a somewhat higher percentage difference in regions where horizontal gradients of EPV were weak, such as along "tongues" of locally high or low EPV. They also found that fields of EPV exhibited good day-to-day conservation, despite the fact that there is little temporal continuity imposed in the method of analysis.

By contrast, Fairlie and O'Neill (1988) documented an example of a major stratospheric warming in which differential advection of EPV in a vertically sheared flow contributed to apparent loss of EPV on a large scale. These contrasting findings emphasize the limitations of gross error statistics as indicators of data quality.

(c) Impact of base level analyses

Fields of geopotential height in the stratosphere are obtained by adding retrieved thicknesses to a base-level analysis of geopotential height at 100 HPa. Substantial improvements have occurred during the past decade in the analyses of the upper troposphere and lower stratosphere produced by the major weather forecasting centres (Bengtsson and Shukla 1988). Operational analysis methods at UKMO, NMC and the European Centre for Medium Range Weather Forecasts (ECMWF) have been documented and intercompared by Hollingsworth et al. (1985). At the three centres, increasing use has been made of asynoptic data, e.g. from aircraft and satellites. There are differences in quality control and analysis methods: e.g. in the treatment of isolated, but quite accurate, synoptic reports, and in the application of spatial smoothing. In addition, problems are caused by delayed reports and regionally sparse data . Tropospheric height analyses for the southern hemisphere are generally poorer than those for the northern (Hollingsworth et al. 1985; Lambert 1988; Trenberth and Olson 1988).

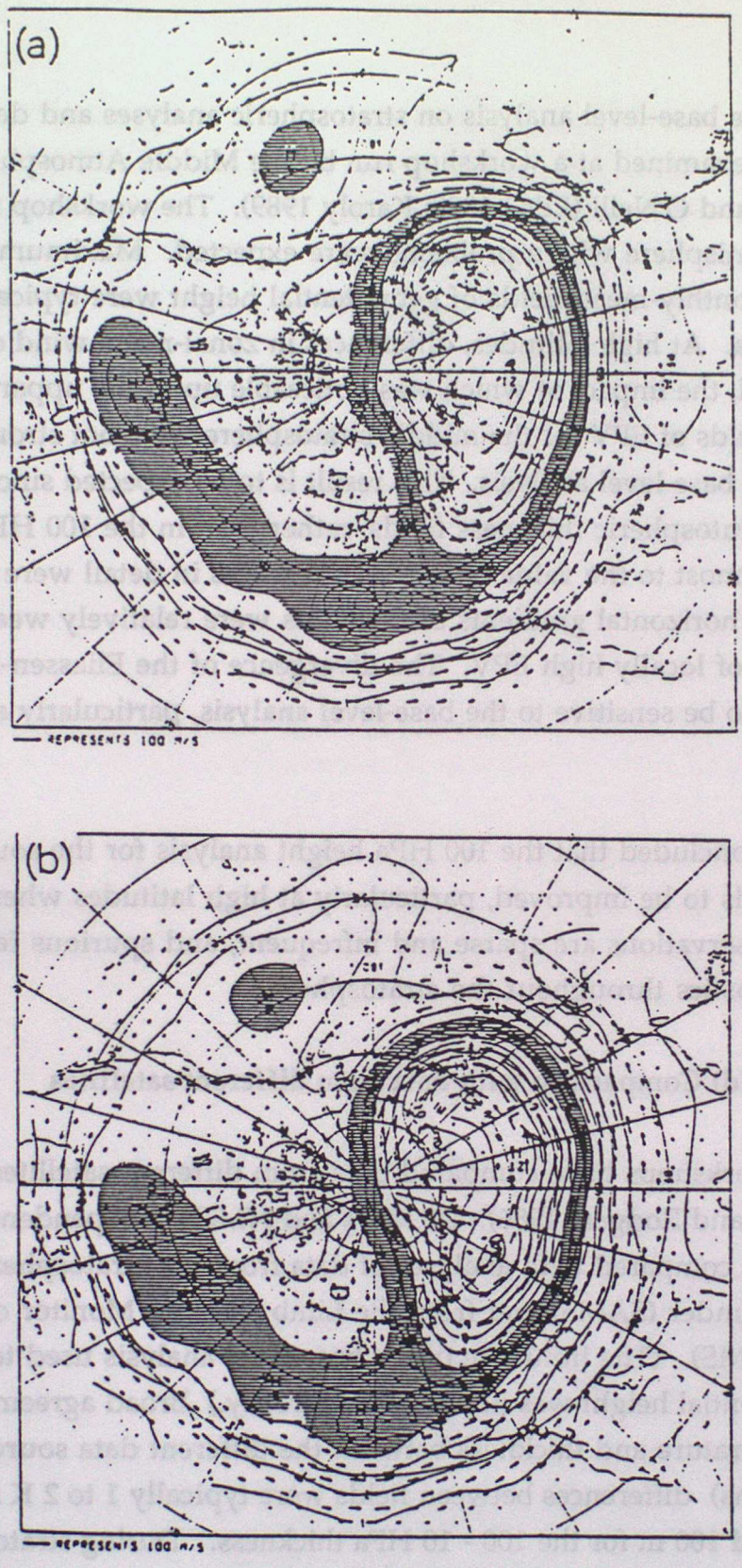

Figure 7 Ertel's potential vorticity and geostrophic winds evaluated on the 850 K isentropic surface for 7 December 1981. (a) Using data from NOAA-6; (b) using data from NOAA-7. Units: 10^{-4} K m^2 kg^{-1}. In these units, areas with values between 4 and 6 are shaded. Reproduced from Clough et al. (1985).

The impact of the base-level analysis on stratospheric analyses and derived diagnostics was examined at a workshop run by the Middle Atmosphere Program (Miles and O'Neill (Eds.) 1989; Karoly 1989). The workshop focused on the southern hemisphere where problems were expected. Maximum regional differences in monthly-mean fields of geopotential height were typically about 100 m at 100 HPa. At high latitudes, differences in zonal-mean wind of up to 15 ms^{-1} were found, the impact of which was noticeable up to the upper stratosphere. Fields of EPV for the middle stratosphere were not strongly affected by differences in base-level analysis. This result is to be expected since horizontal derivatives in stratospheric thickness fields, rather than in the 100 HPa height field, contribute most to the value of EPV. Differences in detail were found, however, where horizontal gradients of thickness were relatively weak, e.g. along "tongues" of locally high EPV. The divergence of the Eliassen-Palm flux was also found to be sensitive to the base-level analysis, particularly at high latitudes.

The workshop concluded that the 100 HPa height analysis for the southern hemisphere needs to be improved, particularly at high latitudes where conventional observations are sparse and infrequent, and spurious features may influence diagnostics throughout the stratosphere.

(d) Comparison with data from different satellites

Several MAP workshops have compared data from different satellites (Rodgers 1984 a, b; Grose and Rodgers 1986). UKMO's and NMC's independent analyses of TOVS data were compared with analyses of data from the Stratospheric and Mesospheric Sounder (SAMS) and from the Limb Infrared Monitor of the Stratosphere (LIMS). (The influence of the base-level analysis used to construct fields of geopotential height was not assessed directly.) Broad agreement was found for temperature and thickness between the different data sources. Root-mean-square (rms) differences between fields were typically 1 to 2 K for temperature, and 100 m for the 100 - 10 HPa thickness. During stratospheric warmings, rms differences were about twice as big. Substantial differences between data sets were found for EPV and the divergence of the Eliassen-Palm flux, quantities that are computed by second order spatial differentiation. The workshops did not identify any systematic differences between the data sources, and did not single out one data source as being better than any other.

4. Conclusions

Since 1978, radiometers on board the TIROS series of operational satellites have taken accurate radiance measurements of the stratosphere over almost the whole globe. These radiances have been processed routinely at the Meteorological Office (UKMO), where a thirteen-year archive of the data has been built up, and continues to be added to. In addition to the radiance measurements themselves, this archive consists of global, gridded analyses of atmospheric thicknesses and of geopotential heights. The thicknesses are retrieved from the radiances by a linear, physical-statistical method; geopotential heights are obtained by adding the thicknesses to a field of geopotential height at 100 HPa. This base-level analysis has come from different weather forecasting agencies over the years. Since 1984, it has been supplied daily, together with analyses at other tropospheric and lower stratospheric levels, as a by-product of operational weather forecasting by UKMO. Analyses of geopotential height are produced on a regular 5° by 5° latitude - longitude grid at the standard pressure levels of 850, 500, 300, 200, 100, 50, 20, 10, 5, 2, 1 HPa. These analyses have formed the basis of numerous diagnostic and modelling studies of the stratosphere. They are available in the U.K. from the Geophysical Data Facility at the Rutherford/Appleton Laboratory, or from UKMO. Some data protocols do apply, but they are mild.

The analysed fields have the advantage of good horizontal resolution, almost global coverage, and long data record. Moreover, for studies covering long periods of time, or for intercomparisons of different years, the data have the distinct advantage of being produced by a processing method that has remained unchanged. The main limitation of the data are its inherently low vertical resolution, which can blur comparatively small-scale baroclinic structures in the stratosphere (especially during strong warmings), and which can lead to discrepancies in diagnostic calculations (O'Neill and Pope 1992), especially when second (or higher) orders of spatial differentiation are involved.

Prospective users of the data should check the following before choosing a period to study:

1. How many missing days or days with poor data coverage there are in the data record for each month (fig. 3).

2. Whether there are any non-operational radiometer channels (table 2 and Fig. 2) and what layers in the stratosphere are affected (Fig. 1(b)).
3. Whether during the period there is a change in the satellite from which the data are obtained (Fig. 2).
4. Whether there is a change in the origin of the tropospheric and 100 HPa analyses of geopotential height (Fig. 4).
5. Whether there were changes in SSU cell pressure (table 1).

The appendix gives details of data formats. When examining data for a particular day, users are advised to check the following indicators of data quality detailed in the appendix:
1. The coverage code, which gives information about the data used to produce the analysis.
2. The number of missing grid points (for gridded data). If this exceeds 650, then consider rejecting that day.
3. Missing data indicators, which show which fields, if any, are missing on a given day.

Although there are advantages in keeping the same processing techniques when building up a data archive, as has been done here, improvements on our methods are now possible, at least in principle. Instead of using a reference set of temperature profiles as *a priori* data in the retrieval of thicknesses, up-to-date fields from a weather forecasting model could be used (Eyre and Lorenc 1989). Instead of gridding retrieved thicknesseses by simple interpolation in space and time, thicknesses could be assimilated into an atmospheric general circulation model, as is commonly done in operational weather forecasting (Lorenc 1986). By making an optimal combination of information from the model and from different measuring instruments, data assimilation should lead to a more accurate, self-consistent and highly resolved view of the atmosphere than can be derived from cruder methods. Better still would be to avoid treating retrieval and assimilation as a two-stage process, and instead to assimilate radiances directly into the model. (To do so, simulated radiances must be calculated form the model's temperature fields, a computationally expensive procedure to do routinely.) Radiometers give very accurate measurements of radiance, so such a method would be ideal theoretically, and is likely to become normal practice before too long.

As part of its involvement in the Upper Atmosphere Research Satellite (UARS) project, the middle atmosphere group at UKMO is using the technique of data assimilation to analyse TOVS temperatures, along with all atmospheric data on the synoptic data bank. (UARS data will be included eventually.) Since October 1991, an archive has been built up for the troposphere and stratosphere in parallel with the archive described in this paper. The analyses are being supplied as "correlative data" to investigators on the UARS project, and will be more widely available in due course.

Annex

Calculation of simulated radiances (section 2.2)

In order to compute equivalent radiances from temperature profiles measured by rockets (as required by the regression analysis described in section 2.2), the combined transmittance of the atmosphere/radiometer system must be known as a function of height. For computational economy, the atmospheric transmittance is parametrized in terms of temperature differences from a reference temperature profile. The parametrization, formulated by McMillin and Fleming (1976, 1977), involves certain "transmission coefficients", which are pre-computed for different zenith angles by detailed radiative transfer calculations for a given set of standard atmospheric temperature profiles. The procedure was as follows:

1. Sixteen standard atmospheric profiles were selected, with one picked as a reference.
2. The combined transmittance of the atmosphere/radiometer system was computed for each of the standard atmospheres combined with each of the radiometer channels. This was done by using Drayson's (1966) technique of line-by-line integration.
3. An approximate formula was then derived, expressing these transmittances as a nonlinear function of temperature differences between atmospheric temperature and the reference temperature profile. The formula involves constant coefficients, called transmission coefficients.
4. By using this formula and its pre-computed transmission coefficients, combined atmosphere/radiometer transmittances were computed as a function of height for each combination of radiometer channel, viewing angle and

temperature profile in the historical set of 1200 profiles used in the regression analysis.

5. Simulated radiances were then derived by integrating through the depth of the atmosphere the product of the Planck function and the vertical derivative of the transmittance. (Each radiance was expressed as a brightness temperature, i.e. the equivalent black-body temperature, by choosing an effective wavenumber for each channel; see Barwell 1977.)

Appendix: Data Formats

A.1 Format of orbital radiance data

A.1.1 Introduction

Each dataset contains one day of daily radiances along satellite orbits. The radiances are often used in the form of equivalent brightness temperatures (code for the conversion is given in A.1.4).

Each set of radiances is for the channels :-

HIRS-2	channel	1	
"	"	2	
"	"	3	
"	"	8	
"	"	9	⌈ see
"	"	17	⌊ note 4
MSU	"	23	
"	"	24	
SSU	"	25	
"	"	26	
"	"	27	

HIRS-2 = High Resolution Infra-Red Sounder Model 2
MSU = Microwave Sounding Unit
SSU = Stratospheric Sounding Unit

The HIRS-2, MSU and SSU satellite radiometers are on board the TIROS-N series of polar orbiter satellites. They scan from side to side across the path of the satellite and take measurements for various fields of view.

Each set of radiances is associated with a particular field of view (FOV) with its own latitude and longitude. There are 4 fields of view (10° and 30° either side of nadir) associated with each scan.

Each record of radiances contains 4 adjacent scans (and therefore a total of 16 fields of view) and covers a time period of 256 seconds.

There are 254 items in a record. Each item is of type integer * 2. Note that the radiances are scaled as indicated in note 5.

Missing data are indicated by the value -32768

A.1.2 Record format

The format of each record is as follows :

Item No	Byte Offset	Description	Comments
1	0	Identifier	22222
2	2	Block sequence number	
3	4	Yearday	YDDD format
4	6	Minutes	
5	8	Tenths of seconds	
6	10	Spacecraft identifier	See note 1
7	12	Unit identifier	See note 2
8	14	No of transverse scans	4
9	16	No of FOV s per scan	4
10	18	No of channels per FOV	11
11	20	No of channels per FOV	11
12	22	Source of data	See note 3
13	24	Orbit number	
14	26	Number of items in record (excluding first 16 items)	238

15	28	Not used	
16	30	Not used	
17	32	Data type	1
18	34	Not used	
19	36	Not used	
20	38	1st channel number	See note 4
21	40	2nd " "	" "
22	42	3rd " "	" "
23	44	4th " "	" "
24	46	5th " "	" "
25	48	6th " "	" "
26	50	7th " "	" "
27	52	8th " "	" "
28	54	9th " "	" "
29	56	10th " "	" "
30	58	11th " "	" "
31	60	Scan number * 100 + FOV number	101 (for first scan and first FOV in that scan)
32	62	Latitude of FOV	In hundredths of degrees (South negative)
33	64	Longitude of FOV	In hundredths of degrees (West negative)
34	66	Radiance for 1st channel	See note 5
35	68	Radiance for 2nd channel	" "
36	70	Radiance for 3rd channel	" "
37	72	Radiance for 4th channel	" "
38	74	Radiance for 5th channel	" "
39	76	Radiance for 6th channel	" "
40	78	Radiance for 7th channel	" "
41	80	Radiance for 8th channel	" "

42	82	Radiance for 9th channel	" "
43	84	Radiance for 10th channel	" "
44	86	Radiance for 11th channel	" "

Items 45 to 86 are a repeat of items 31 to 44 for the other 3 FOV s in the first scan.

Items 87 to 254 are a repeat of items 31 to 86 for the other 3 scans in the record.

A.1.3 Notes

Note 1 : The spacecraft identifier (item 6) is a code with value 2^{n-1}, where

n	=	1	=	TIROS-N
		2	=	NOAA-6
		4	=	NOAA-7
		5	=	NOAA-9
		6	=	NOAA-8
		8	=	NOAA-11

Note 2 : The unit identifier (item 7) is a code for the sounding units used to obtain the radiances and hence thicknesses.

1	=	HIRS-2
2	=	MSU
4	=	SSU

Combinations of sounding units are indicated by adding code values. Usually all 3 sounding units are used - in which case the unit identifier equals 1 + 2 + 4 = 7.

Note 3 : The source of data (item 12) identifies the process which produced the radiances.

1 = processed by NOAA/NESDIS

Note 4 : Channel number (items 20-30) - they are not necessarily in numerical order in the dataset.

0	=	No channel	
1	=	HIRS-2 channel	1
2	=	" "	2
3	=	" "	3
8	=	" "	8
9	=	" "	9
17	=	" "	17
23	=	MSU "	23
24	=	" "	24
25	=	SSU "	25
26	=	" "	26
27	=	" "	27

On some occassions HIRS 2 channels 9 and 17 have been replaced by MSU channels 21 and 22 respectively.

Note 5 : The radiance values (items 34-44) are in units of mW/(cm^{-1} Sr m^2) and are scaled as follows :

Channel	Scaling factor
1	x 64
2	"
3	"
8	"
9	"
17	x 4096
21	x 262144
22	"
23	"
24	"
25	x 64
26	"
27	"

The true radiance value = radiance value in dataset divided by the scaling factor.

A.1.4 Coversion of radiances to brightness temperatures

Equivalent brightness temperatures are derived from the true radiance values (see note 5) using the following FORTRAN code :

```
ALPHA = 1.19094E-5 * (WV**3)
BETA = 1.43879 * WV
BRIGHT = BETA/ALOG(ALPHA/RAD + 1.0)
```

where

WV = the "effective wavenumber" for the given channel (see below)
RAD = radiance
BRIGHT = brightness temperature

Channel	"Effective wavenumber"
23	1.832
24	1.932
25	669.99
26	669.63
27	669.34

The "effective wavenumber" for a HIRS-2 channel varies with spacecraft and can be supplied on request.

A.2 Format of SSU orbital thickness datasets

A.2.1 Introduction

Each dataset contains one day of stratospheric thicknesses along satellite orbits. Thicknesses are for the layers :-

100 - 20	HPa
100 - 10	"
100 - 5	"
100 - 2	"
100 - 1	"

The thicknesses are derived from combinations of radiances as measured by the HIRS-2, MSU and SSU satellite radiometers (see section 2 for description of the retrieval method). These instruments scan from side to side across the path of the satellite and take measurements for various fields of view.

Each set of thicknesses is associated with a particular field of view at a particular latitude and longitude. There are 4 fields of view (FOV) for each scan (10° and 30° either side of nadir).

Each record of thicknesses contains 4 adjacent scans (and therefore a total of 16 fields of view) and covers a time period of 256 seconds.

There are 152 items in a record. Each item is of type integer * 2. Note that the thicknesses are scaled as indicated in note 4.

Missing data are indicated by the value -32768

A.2.2 Data format

The format of each record is as follows :

Item No	Byte Offset	Description	Comments
1	0	Identifier	22222
2	2	Block sequence number	
3	4	Yearday	YDDD format
4	6	Minutes	
5	8	Tenths of seconds	
6	10	Spacecraft identifier	See note 1
7	12	Unit identifier	" " 2
8	14	No of transverse scans	4
9	16	No of FOV s per scan	4
10	18	No of thicknesses per FOV	5
11	20	No of thicknesses per FOV	5
12	22	Source of data	See note 3
13	24	Orbit number	
14	26	No. of items in record (excluding first 16 items)	136
15	28	Not used	
16	30	Not used	
17	32	Data type	8
18	34	Not used	
19	36	Not used	
20	38	Code number for 100 - 20 HPa layer	502
21	40	Code number for 100 - 10 HPa layer	503
22	42	Code number for 100 - 5 HPa layer	504
23	44	Code number for 100 - 2 HPa layer	505
24	46	Code number for 100 - 1 HPa layer	506

25	48	Scan number * 100 + FOV number	101 (for first scan and first FOV in that scan)
26	50	Latitude of FOV	In hundredths of degrees (South negative)
27	52	Longitude of FOV	In hundredths of degrees (West negative)
28	54	100 - 20 HPa thickness	See note 4
29	56	100 - 10 HPa thickness	" "
30	58	100 - 5 HPa thickness	" "
31	60	100 - 2 HPa thickness	" "
32	62	100 - 1 HPa thickness	" "

Items 33 to 56 are a repeat of items 25 to 32 for the other 3 FOV s in the first scan.

Items 57 to 152 are a repeat of items 25 to 56 for the other 3 scans in the record.

A.2.3 Notes

Note 1 : The spacecraft identifier (item 6) is a code with value 2^{n-1} , where

n	=	1	=	TIROS-N
		2	=	NOAA-6
		4	=	NOAA-7
		5	=	NOAA-9
		6	=	NOAA-8
		8	=	NOAA-11

Note 2 : The unit identifier (item 7) is a code for the sounding units used to obtain the radiances and hence thicknesses.

1	=	HIRS-2
2	=	MSU
4	=	SSU

Combinations of sounding units are indicated by adding code values. Usually all 3 sounding units are used - in which case the unit identifier equals 1 + 2 + 4 = 7.

Note 3 : The source of data (item 12) identifies the process which produced the thicknesses.
5 = Retrieved data

Note 4 : The thickness values (items 28-32) are in units of decametres and are scaled by a factor of 5. The true thickness value in metres = thickness value in dataset x 2.

A.3 Format of SSU monthly radiance datasets

A.3.1 Introduction

Each dataset contains analysed atmospheric radiances from a number of radiance channels on a global grid for each day in a month. The radiances are for the following radiometer channels :

HIRS 2	channel	1	
"	"	2	
"	"	3	
"	"	8	
"	"	9	⌈ see
"	"	17	⌊ note 2
MSU	"	23	
"	"	24	
SSU	"	25	
"	"	26	
"	"	27	

The global grid is a regular latitude - longitude grid of grid length 5°. There are 37 latitudes from 90°N to 90°S and 72 longitudes from 180°W to 175°E.

The radiances are obtained from analysis of radiances supplied on an orbital grid by NOAA/NESDIS (as described in section 2.2 stage 2.6).

Each day's data consists of 38 records. The first record contains header information about the data while the other 37 records contain the radiances. The days are in chronological order.

There are 1080 items in each record. Each item is of type integer * 2. Note that data are scaled as indicated in note 4.

Missing data are indicated by the value -32768.

The formats of the 38 records are as follows :

A.3.2 Format of first (header) record

Item No	Byte Offset	Description	Comments
1	0	Grid type	3 - global grid
2	2	No of columns in grid	72
3	4	No of rows in grid	37
4	6	1st channel number	See note 2
5	8	2nd " "	" "
6	10	3rd " "	" "
7	12	4th " "	" "
8	14	5th " "	" "
9	16	6th " "	" "
10	18	7th " "	" "
11	20	8th " "	" "
12	22	9th " "	" "
13	24	10th " "	" "
14	26	11th " "	" "
15	28	Not used	
16	30	Year/month	mm + (yy * 100)
		(year = true year - 1900)	
17	32	Day/hour	hh + (dd * 100)
18	34	Analysis time window	720 minutes

19	36	Data flag for 1st channel number	0 = invalid data 1 = valid data

Items 20 to 30 are as item 19 but for the other channels. The order of the flags is the same as the order of the channel numbers.

31	60	Hemisphere covered	0 = global
32	62	Number of fields of view per record of orbital radiance data used in analysis	16
33	64	Number of radiance records used in analysis	Variable (0 = no data)
34	66	Spacecraft code	See note 1
35	68	Search radius used for individual fields of view in analysis.	500 km
36	70	Search radius used for a record of radiances used in analysis.	900 km
37	72	Anaysis time window	720 minutes
38	74	Background weighting in hundredths	0 = no background
39	76	Number of grid points with no fields of view within search radius.	Variable, see note 3 (2664 = no data)
40	78	Number of smoothing vectors used in smoothing analysed data.	25
41	80	Not used	
42	82	Not used	
43	84	Not used	

Items 44 to 1080 are not used and are set to 0

A.3.3 Format of second (data) record

The data is for row 1 (90°N) of the lat - long grid

Item No	Byte Offset	Description	Comments
1	0	Not used	Set to -32768
2	2	Not used	Set to -32768
3	4	Not used	Set to -32768
4	6	1st channel radiance for 1st longitude (180°W)	See notes 4 and 5

Items 5 to 14 are the same as item 4 but for the 2nd. to 11th channels.

15	28	Not used	

Items 16 to 30 are the same as items 1 to 15 but for the 2nd. longitude (175°W) of the 90°N latitude circle.

Similarly, items 31 to 1080 are for the 3rd. to 72nd. longitudes (170°W to 175°E) respectively of the 90°N latitude circle.

A.3.4 Format of third to 38th (data) records

The format of each of these records is the same as that of the second record except that the data is for the 2nd (85°N) to the 37th (90°S) latitudes of the lat-long grid.

A.3.5 Notes

Note 1 : The spacecraft identifier (item 34 of header) is a code with value 2^{n-1}, where

n	=	1	=	TIROS-N
		2	=	NOAA-6
		4	=	NOAA-7

5	=	NOAA-9
6	=	NOAA-8
8	=	NOAA-11

Note 2 : The channel number (item 4 of header) indicates one of the following channels :

Channel number	Channel			
1	HIRS-2	channel	1	
2	"	"	2	
3	"	"	3	
8	"	"	8	
9	"	"	9	⌈ see
17	"	"	17	⌊ below
23	MSU	"	23	
24	"	"	24	
25	SSU	"	25	
26	"	"	26	
27	"	"	27	

For certain periods HIRS 2 channels 9 and 17 are replaced by MSU channels 21 and 22.

Note 3 : The number of grid points with no fields of view within the search radius (item 39) gives an indication of the accuracy of the analysis. If there are more than 650 missing grid points it is recommended that the analysis is not used.

Note 4 : The radiance values (main items in data records) are in units of $mW/(cm^{-1}\ Sr\ m^2)$ and are scaled by a factor which depends on the channel.

Channel	Scaling factor
1	x 64
2	"
3	"

8	"
9	"
17	x 4096
21	x 262144
22	"
23	"
24	"
25	x 64
26	"
27	"

True radiance value = radiance value in dataset / scaling factor

Note 5 : True radiances can be converted to equivalent brightness temperatures using the FORTRAN code detailed in section A.1.4.

Note 6 : Dataset names are as follows :

M20.SnnRAD#3.YyyMmmG

where	nn	=	Spacecraft number
		=	01 for TIROS-N
		=	02 for NOAA-6
		=	04 for NOAA-7
		=	05 for NOAA-9
		=	06 for NOAA-8
		=	08 for NOAA-11
	yy	=	Year - 1900
	mm	=	Month
	G	=	Generation number
		=	1 = data from SSU radiance channels only
		=	2 = data from all radiance channels

N.B. The monthly radiance dataset is constructed from daily radiance datasets. Each of these datasets has its own generation number. The generation number used in the monthly radiance dataset name is set equal to the most common generation number amongst the daily radiance datasets.

Note 7 : The datasets are organised on tape into blocks of records of fixed length. The blocksize = 21600 bytes and the record length = 2160 bytes.

A.4 Format of the SSU monthly heights datasets

A.4.1 Introduction

Each dataset contains analysed tropospheric and stratospheric geopotential heights on a global grid for each day in a month.

The heights are for the levels :-

850 500 300 200 100 50 20 10 5 2 1 HPa

The global grid is a regular latitude - longitude grid of grid length 5°. There are 37 latitudes from 90°N to 90°S and 72 longitudes from 180°W to 175°E.

The tropospheric heights (up to and including the 50 HPa level) are obtained from an operational global analysis, while the stratospheric heights are calculated from the 100 HPa operational analysis heights and sets of thicknesses on an orbital grid. The latter are retrieved from orbital radiances as measured by HIRS-2, MSU and SSU sounding units.

Each day's data consists of 38 records. The first record contains header information about the data, while the other 37 records contain the heights. The days are in chronological order.

There are 1080 items in each record. Each item is of type integer * 2. Data are scaled as indicated in note 4.

Missing data are indicated by the value -32768.

The formats of the 38 records are as follows :

A.4.2 Format of first (header) record

Item No	Byte Offset	Description	Comments
1	0	Grid type	3 - global grid
2	2	No of columns (longitudes) in grid	72
3	4	No of rows (latitudes) in grid	37
4	6	1st pressure level (HPa)	1000 (not used)
5	8	2nd " " "	850
6	10	3rd " " "	500
7	12	4th " " "	300
8	14	5th " " "	200
9	16	6th " " "	100
10	18	7th " " "	50
11	20	8th " " "	20
12	22	9th " " "	10
13	24	10th " " "	5
14	26	11th " " "	2
15	28	12th " " "	1
16	30	Year/month (year = true year - 1900)	mm + (yy * 100)
17	32	Day/hour	hh + (dd * 100) hh = 0 GMT before 3/8/79 12 GMT from 3/8/79
18	34	Analysis time window	720 minutes
19	36	Data flag for 1000mb	0 = invalid data 1 = valid data 2 = interpolated data 3 = thicknesses

Items 20 to 30 are as item 19 but for the other heights. The order of the flags is the same as the order of the pressure levels.

31	60	Hemisphere covered	0 =global
32	62	Number of fields of view per record of orbital thickness data used in analysis	16
33	64	Number of thickness records used in analysis	Variable
34	66	Spacecraft code	See note 1
35	68	Search radius used for individual fields of view in analysis.	500 km
36	70	Search radius used for a record of thicknesses used in analysis.	900 km
37	72	Anaysis time window	720 minutes
38	74	Background weighting in hundredths	0 = no background
39	76	Number of grid points with no fields of view within search radius.	Variable see note 2
40	78	Number of smoothing vectors used in smoothing analysis.	25 (i.e. truncation at zonal wave 12)
41	80	Coverage code	See note 3
42	82	Time of tropospheric data	usually, but not always, the same as hh in item 17
43	84	Interpolation of 50 HPa data	0 = actual data 1 = interpolated data

Items 44 to 1080 are not used and are set to 0

A.4.3 Format of second (data) record

The data is for row 1 (90°N) of the lat - long grid

Item No	Byte Offset	Description	Comments

1	0	Not used	Set to -32768
2	2	Not used	Set to -32768
3	4	Not used	Set to -32768
4	6	1000 HPa heights for 1st. longitude (180°W)	Not used. Set to -32768
5	8	850 HPa heights for 1st. longitude (180°W)	See note 4

Items 6 to 15 are the same as item 5 but for pressure levels 500, 300, 200, 100, 50, 20, 10, 5, 2 and 1 HPa.

Items 16 to 30 are the same as items 1 to 15 but for the 2nd. longitude (175°W) of the 90°N latitude circle.

Similarly, items 31 to 1080 are for the other longitudes (170°W to 175°E) of the 90°N latitude circle.

A.4.4 Format of 3rd. to 38th (data) records

The format of each of these records is the same as that of the 2nd. record except that the data is for latitudes 85°N to 90°S.

A.4.5 Notes

Note 1 : The spacecraft identifier (item 34) is a code with value 2^{n-1} , where

n	=	1	=	TIROS-N
		2	=	NOAA-6
		4	=	NOAA-7
		5	=	NOAA-9
		6	=	NOAA-8
		8	=	NOAA-11

Note 2 : The number of grid points with no fields of view within the search radius (item 39) gives an indictation of the accuracy of the analysis. If there are more than 650 missing grid points it is recommended that the analysis is not used.

Note 3 : The coverage code (item 41) gives information about the data used to produce the height analysis.

0	=	NMC + THK#3 thicknesses(Global)
1	=	NMC only (Global)
2	=	UKMO(NH) + THK#3 thicknesses (N Hemi) THK#3 100 HPa + THK#3 thicknesses (S. Hemi)
3	=	UKMO(NH) + THK#3 thicknesses (N Hemi) THK#3 thicknesses only (S Hemi)
4	=	UKMO(NH) only
5	=	THK#3 100 HPa + THK#3 thicknesses (Global)
6	=	THK#3 thicknesses only (Global)
7	=	No data
8	=	ECMWF + THK#3 (Global)
9	=	ECMWF only (Global)
10	=	UKMO(GL) or UKMO(UM) + THK#3 (Global)
11	=	UKMO(GL) or UKMO(UM) only (Global)

NMC	=	analysed tropospheric heights (850, 500, 300, 100 and 50 HPa) from NMC (Washington).
THK#3 thicknesses	=	analysed stratospheric thicknesses (100 - 20, 100 - 10, 100 - 5, 100 - 2 and 100 - 1 HPa).
UKMO	=	analysed tropospheric heights (850, 500, 300, 100 and 50 HPa) from the UK Meteorological Office operational analysis.
UKMO(NH)	=	For coverage codes 2, 3 and 4, the UKMO tropospheric heights were produced for the northern hemisphere only using the hemispheric Octagon model.
UKMO(GL)	=	Before 12 June 1991, for coverage codes 10 and 11, the UKMO analyses were produced with the first global weather forecasting model (GL) at UKMO.
UKMO(UM)	=	After 12 June 1991, for coverage codes 10 and 11, the UKMO analyses were produced with the new weather forecasting model at UKMO, the Unified Model (UM).

THK#3 100 HPa	=	analysed heights at 100 HPa from NMC (Washington).
ECMWF	=	analysed tropospheric heights (850, 500, 300, 100 and 50 HPa) from ECMWF.
N Hemi	=	data from 90°N to approximately 20°N.
S Hemi	=	data from approximately 20°N to 90°S.

Note 4 : The heights (main items in data records) are written in decametres and are scaled by a factor of 5. The true height in metres = height value in dataset x 2.

Note 5 : Dataset names are as follows :

M20.SnnHTS#3.YyyMmmG

where nn = Spacecraft number
= 01 for TIROS N
= 02 for NOAA 6
= 04 for NOAA 7
= 05 for NOAA 9
= 06 for NOAA 8
= 08 for NOAA 11

yy = Year - 1900
mm = Month
G = Generation number
= 1 data from SSU radiance channels only
= 2 data from all radiance channels

N.B. The monthly heights dataset is constructed from daily heights datasets. Each of these datasets has its own generation number. The generation number used in the monthly heights dataset name is set equal to the most common generation number amongst the daily heights datasets.

Note 6 : The datasets are organised on tape into blocks of records of fixed length. The blocksize = 21600 bytes and the record length = 2160 bytes.

References

Barwell, B.R. 1977 Optimum choice of equivalent wavenumber for a satellite radiometer with finite bandwidth. U.K. Meteorological Office, Met O 19 Branch Memorandum, No. 41.

Bengtsson, L. and Shukla, J. 1988 Integration of space and insitu observations to study global climate change. Bull. Amer. Meteorol. Soc., **69**, 1130-1143.

Campbell, J.S. and Pick, D.R. 1979 Retrieval of stratospheric data from the sounders on the TIROS-N series of operational satellites during the first year of operation. U.K. Meteorological Office, Met O 19 Branch Memorandum, No. 54.

Clough, S.A., Grahame, N.S.. and O'Neill, A. 1985 Potential vorticity in the stratosphere derived using data from satellites. Quart. J. Roy. Meteorol. Soc., **111**, 335-358.

Drayson, S.R. 1966 Atmospheric transmission in the CO_2 bands between 12m and 18m. Appl. Optics, **5**, 385-391.

Eyre, J.R. and Lorenc, A.C. 1989 Direct use of satellite sounding radiances in numerical weather prediction. Met. Mag., **118**, No. 1398, 13-16.

Fairlie, T.D.A.and O'Neill, A. 1988 The stratospheric major warming of winter 1984/85: Observations and dynamical inferences. Quart.J. Roy. Meteorol. Soc., **114**, 557-578.

Fairlie, T.D.A., Fisher, M. and O'Neill, A. 1990 The development of narrow baroclinic zones and other small-scale structure in the stratosphere during simulated major warmings. Quart. J. Roy. Meteorol. Soc., **116**, 287-315.

Grose, W.L. and Rodgers, C.D. 1986 Coordinated study of the behavior of the middle atmosphere in winter: monthly-mean comparisons of satellite and radiosonde data and derived quantities. MAP handbook, **21**, 79-111.

Hirota, I. Hirooka, T. and Shiotani, M. 1983 Upper stratosphere circulations in the two hemispheres observed by satellites. Quart. J. Roy. Meteorol. Soc, **109**, 443-454.

Hollingsworth, A. Lorenc, A.C, Tracton, M. S, Arpe,K., Cats, G., Uppala, S., and Kallberg, P. 1985 The response of numerical weather prediction systems to FGGE level IIb data. PartI: Analysis. Quart. J. Roy. Meteorol. Soc., **111**, 1-66.

Jackson, D.R., Harwood, R.S. and Renshaw. E. 1990 Tests of a scheme for regression retrieval and time-space interpolation of stratospheric temperature from satellite measurements. Quart. J. Roy. Meteorol. Soc, **116**, 1449-1470.

Jenkins, D.B., Wareing, D.P., Thomas, L. and Vaughan, G. 1987 Upper stratospheric and mesospheric temperatures derived from lidar observations at Aberystwyth. J. Atmos. Terr. Phys., **49**, No. 3, 287-298.

Karoly, D.J. 1989 The impact of base level analyses on stratospheric circulation statistics. Pure Appl. Geophys., **130**, 181-194.

Labitzke, K., Lenschow, R., Naujokat, B. and Petzoldt, K. 1981 The third winter of PMP-1, 1980/81: A winter with record breaking temperatures. Beilage zue Berliner Wetterkarte. Institute fur Meteorologie, Free University of Berlin, Berlin.

Lambert, S.J. 1988 A comparison of operational global analyses from the European Centre for Medium Range Weather Forecasts (ECMWF) and the National Meteorological Centre (NMC). Tellus, **40A**, 272-284.

Lorenc, A.C. 1986 Analysis methods for numerical weather prediction. Quart. J. Roy. Meteorol. Soc., **112**, 1177-1194.

McIntyre, M.E.and Palmer, T. N. 1983 Breaking planetary waves in the stratosphere. Nature, **305**, 593-600.

McMillin, L.M. and Fleming, H. E. 1976 Atmospheric transmittances of an absorbing gas: a computationally fast and accurate transmittance model for absorbing gases with constant mixing ratios in homogeneous atmospheres. Appl. Optics, **15**, 358-363.

McMillin, L.M. and Fleming, H.E. 1977 Atmospheric transmittance of an absorbing gas 2: a computationally fast and accurate transmittance model for slant paths at different zenith angles. Appl. Optics, **16**, 1366-1370.

Miles, T. and O'Neill, A. 1989 Comparison of satellite-derived dynamical quantities for the stratosphere of the southern hemisphere. MAP handbook, **29**, 245-271.

Nash, J and Brownscombe, J.L. 1983 Validation of the stratospheric sounding unit. Adv. Space Res., **2**, No. 6, 59-62.

Nash, J and Edge, P.R. 1989 Temperature changes in the stratosphere and lower mesosphere 1979-1988 inferred from TOVS radiance observations. Adv. Space Res., **9**, No. 7, 333-341.

Nash, J. and Forrester, G.F. 1986 Long-term monitoring of stratospheric temperature trends using radiance measurments obtained by the TIROS-N series of NOAA spacecraft. Adv. Space Res., **6**, No. 10, 37-44.

O'Neill, A. and Pope, V.D. 1992 The effects of resolution on diagnostic calculations of the coupling between radiation and dynamics. Adv. Space Res., to appear.

Phillips, N., McMillin, L., Gruber, A. and Wark, D. 1979 An evaluation of early operational temperature soundings from TIROS-N. Bull. Amer. Meteorol. Soc., **60**, 1188-1197.

Pick, D.R. and. Brownscombe, J.L 1981 Early results based on the stratospheric channels of TOVS on the TIROS-N series of operational satellites. Adv. Space Res., **1**, 247-260.

Rodgers, C.D. 1984a Workshop on comparison of data and derived dynamical quantities during northern hemisphere winters. Adv. Space Res., **4**, 117-125.

Rodgers, C.D. (Ed.) 1984b Coordinated study of the behaviour of the middle atmosphere in winter (PMP-1). MAP handbook, **12**, 154pp..

Schwalb, A. 1978 The TIROS-N/NOAA A-G satellite series. NOAA Technical Memorandum, NESS 95

Smith, W.L., Woolf, H.M, Hayden, C.M, Wark, D.Q., and McMillin, L.M. 1979 The TIROS-N operational vertical sounder. Bull. Amer. Meteorol. Soc., **60**, 1177-1187.

Trenberth, K.E. and Olson, J.G. 1988 An evaluation and intercomparison of global analyses from the National Meteorological Center. Bull. Amer. Meteorol. Soc., **69**, 1047-1057.

Ziemke, J.R. and Stanford, J.L. 1991 One-to-two month oscillations: observed high-latitude tropospheric and stratospheric response to tropical forcing. J. Atmos. Sci., **48**, No.11, 1336-1347.

CLIMATE RESEARCH TECHNICAL NOTES

CRTN 1	Oct 1990	Estimates of the sensitivity of climate to vegetation changes using the Penman-Monteith equation. P R Rowntree
CRTN 2	Oct 1990	An ocean general circulation model of the Indian Ocean for hindcasting studies. D J Carrington
CRTN 3	Oct 1990	Simulation of the tropical diurnal cycle in a climate model. D P Rowell
CRTN 4	Oct 1990	Low frequency variability of the oceans. C K Folland, A Colman, D E Parker and A Bevan
CRTN 5	Dec 1990	A comparison of 11-level General Circulation Model Simulations with observations in the East Sahel. K Maskell
CRTN 6	Dec 1990	Climate Change Prediction. J F B Mitchell and Qing-cun Zeng
CRTN 7	Jan 1991	Deforestation of Amazonia - modelling the effects of albedo change. M F Mylne and P R Rowntree
CRTN 8	Jan 1991	The role of observations in climate prediction and research. D J Carson
CRTN 9	Mar 1991	The greenhouse effect and its likely consequences for climate change. D J Carson
CRTN 10	Apr 1991	Use of wind stresses from operational N.W.P. models to force an O.G.C.M. of the Indian Ocean. D J Carrington
CRTN 11	Jun 1991	A new daily Central England Temperature series, 1772-1991. D E Parker, T P Legg and C K Folland
CRTN 12	Jul 1991	Causes and predictability of Sahel rainfall variability. D P Rowell, C K Folland, K Maskell, J A Owen, M N Ward
CRTN 13	Jul 1991	Modelling changes in climate due to enhanced CO_2, the role of atmospheric dynamics, cloud and moisture. C A Senior, J F B Mitchell, H Le Treut and Z-X Li

CLIMATE RESEARCH TECHNICAL NOTES

CRTN 14	Sep 1991	Sea temperature bucket models used to correct historical SST data in the Meteorological Office. C K Folland
CRTN 15	Aug 1991	Modelling climate change, and some potential effects on agriculture in the U.K. P R Rowntree, B A Callander and J Cochrane
CRTN 16	Aug 1991	The Boreal Forests and Climate G Thomas and P R Rowntree
CRTN 17	Aug 1991	Development of a Stratosphere-Troposphere Data Assimilation System. R Swinbank.
CRTN 18	Sep 1991	A study of asynchronous coupling using a simple climate model. M K Davey.
CRTN 19	Sep 1991	The Oceanic Carbon Cycle. N K Taylor
CRTN 20	Nov 1991	Worldwide ocean-atmosphere surface fields in Sahel wet and dry years using provisionally corrected surface wind data. M N Ward
CRTN 21	Dec 1991	Coupled tropical ocean global atmosphere models at the UKMO. M K Davey, C Gordon, S Ineson and S Lawrence
CRTN 22	Dec 1991	Empirical parameterisation of tropical ocean-atmosphere coupling. M Allen, M K Davey, D L T Anderson and P D Killworth
CRTN 23	Feb 1992	The temporal evolution of Equatorial Currents in the Indian Ocean D L T Anderson, D J Carrington, R A Corry and C Gordon